Investigation of Narrow Pore Size Distribution on Carbon Dioxide Capture of Nanoporous Carbons

Long-Yue Meng and Soo-Jin Park*

Korea CCS R&D Center, Korea Institute of Energy Research, Daejeon 305-343, Korea
*Department of Chemistry, Inha University, Incheon 402-751, Korea. *E-mail: sjpark@inha.ac.kr*

Nanoporous carbons with a high specific surface area were prepared directly from thermoplastic acrylic resin as carbon precursor and MgO powder as template by carbonization over the temperature range, 500-1000 °C. The effect of the carbonization temperature on the pore structure and CO_2 adsorption capacity of the obtained porous carbon was examined. The textural properties and morphology of the porous carbon materials were analyzed by N_2/−196 °C and CO_2/0 °C adsorption/desorption isotherms, SEM and TEM. The CO_2 adsorption capacity of the prepared porous carbon was measured at 25 °C and 1 bar and 30 bar. The specific surface area increased from 237 to 1251 m^2/g, and the total pore volumes increased from 0.242 to 0.763 cm^3/g with increasing the carbonization temperature. The carbonization temperature acts mainly by generating large narrow micropores and mesopores with an average pore size dependent on the level of carbonization of the MgO-templated nanoporous carbons. The results showed that the MgO-templated nanoporous carbons at 900 °C exhibited the best CO_2 adsorption value of 194 mg/g at 1 bar.

Key Words : Nanoporous carbons, Narrow pore size, CO_2 capture, Carbonization temperature

Introduction

Recently, all developed countries have been concerned with decreasing the level of CO_2 emissions to address the consequences of climate change. Fossil fuels supply more than 98% of the world's energy needs but the combustion of fossil fuels is one of the major sources of the green house gas, CO_2. CO_2 capture from fossil fuels power plants by adsorption and sequestration in unalienable coal seams can be a near-term method of reducing the atmospheric emissions of this greenhouse gas.[1-4]

A range of processes including liquid solvent absorption, cryogenic techniques, membrane separation, solid sorbents, pressure swing adsorption, and temperature swing adsorption have been proposed for CO_2 capture and sequestration by power plants.[4-6] Pressure or temperature swing adsorption technologies can reduce the high cost of gas separation. Up to now, commercial CO_2 capture plants employ amine-based processes and wet scrubbing systems.[7] These processes are energy intensive due to the large amount of water required in these systems and amine degradation by oxidation leading to the corrosion of process equipment.[7-9] The development of more efficient CO_2 adsorption is a pressing requirement to meet the future societal and environmental needs. This demand for more sustainable, efficient CO_2 capture has prompted renewed scientific and government interest in advanced adsorbent designs.

CO_2 from flue gas may be removed using a variety of novel porous solids including porous carbonaceous materials, zeolites, alumina, silica sels, metal-organic frameworks (MOFs), and porous organic polymers.[10-15] Zeolites, mesoporous silica, and MOFs show negligible CO_2 adsorption at 300 °C due to their surface chemistry and structural instability. Nanoporous carbon as a non-oxide porous material has great scientific and technological applications in CO_2 adsorption.

Previous studies evaluated the use of porous carbons as adsorbents for gas adsorption including activated carbon, activated carbon fibers, carbon molecular sieves, carbon nanotubes, graphite nanofibers and graphene.[16-22] In particular, activated carbon has been used in CO_2 adsorption for many years due to their highly developed porosity, extended specific surface area, hydrophobicity of their surface chemistry, thermal stability, and low cost. Recently, methods used for the design of novel nanoporous carbons also need to satisfy the requirements of global energy and environment problems.

In general, activated carbons are usually obtained *via* carbonization of precursors of natural or synthetic origin, followed by activation. It is widely agreed among investigators that the pore structure and the pore size distribution activated carbons are influenced by the starting materials and template.[23-25] And, the carbonization process also plays an important role on the final product and careful selection of carbonization parameters for prepares the required carbons. Among the classical parameters that can be affect its pore structure, one of which is the carbonization temperature seem to be those in which the micro-/meso-porosity of the as-prepared carbons.

From several years ago, the MgO-template method has attracted considerable attention for the preparation of porous carbons. Especially, compare with the conventional template method, MgO has following advantages: (a) MgO template is easily removed by a diluted non-corrosive acid; (b) MgO template can be recycled for the present method; (c) the textural properties of the prepared carbons are tunable by

3750   *Bull. Korean Chem. Soc.* **2012**, Vol. 33, No. 11

Long-Yue Meng and Soo-Jin Park

changing MgO size and carbon precursor.[26]

In this study, nanoporous carbons with a high specific surface area were prepared directly from a thermoplastic acrylic resin and MgO by carbonization at 500-1000 °C. This method has been used to enhance the porosity of the carbon materials, and develop their CO_2 adsorption capacities.

Experimental

The thermoplastic acrylic resin (Sumyoung Co.) was impregnated with MgO (Aldrich, 10-15 nm) at carbonization temperatures of 500, 700, 800, 900, and 1000 °C. For example, 1 g of resin was mixed with 2 g of MgO. The mixture was placed in a quartz tube reactor, heated to 500 °C at a rate of 5 °C/min in N_2 flow (200 mL/min) and kept at this temperature for 2 h before cooling to room temperature. The carbonized product was washed with 5 wt % HCl and hot distilled water, filtered and dried at 100 °C. The sorbents are denoted as M-500, M-700, M-800, M-900, and M-1000, respectively. For comparison, the pristine resin was placed in a quartz tube reactor, heated to 900 °C at a rate of 5 °C /min in N_2 flow (200 mL/min) and kept at this temperature for 2 h before cooling to room temperature. The obtained powder was denoted as M-0.

The textural properties of the samples were determined by physically adsorbing N_2/−196 °C and CO_2/0 °C using a surface area analyzer (BEL, Japan). Before the experiment, the samples were degassed at 200 °C to a constant pressure of 10^{-4} Torr. The isotherms were used to calculate the specific surface area, micropore volume, mesopore volume, total pore volume, and pore size distribution. The morphologies of the samples were analyzed by scanning electron microscopy (SEM, Hitachi S-4200) and transmission electron microscopy (TEM, JEM2100F, JEOL).

The CO_2 adsorption test was conducted under ambient conditions of 25 °C at both low (1 bar) and moderate pressures (30 bar, BEL, Japan). In each experiment, approximately 0.1 g of the sample was loaded into a stainless chamber. Before the measurements, the samples were degassed at 300 °C for 12 h to obtain a residual pressure of 10^{-4} Torr. After the chamber was cooled to room temperature, CO_2 was introduced until the pressure reached 30 bar. Ultrahigh purity grade (99.9999%) CO_2 was used so that the effects of moisture and other impurities could be excluded. Finally, a volumetric measurement method was used to determine the CO_2 adsorption capacity.

Results and Discussion

Figure 1 shows the adsorption/desorption isotherms of N_2 on all samples at −196 °C. The adsorption/desorption isotherms of M-500, M-700, and M-1000 showed Type IV isotherms according to the IUPAC classification. The adsorption/desorption isotherms for M-800 and M-900 corresponds to Type I isotherms according to the IUPAC classification. On the other hand, the isotherms of M-0 showed a
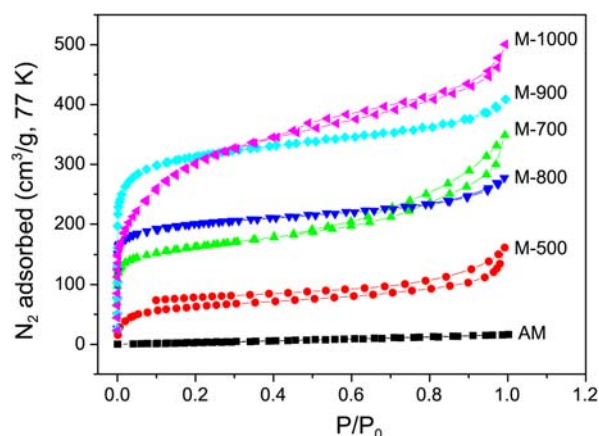

Figure 1. The N_2 full isotherms of the prepared nanoporous carbons.

line shape. This means that M-0 has the characteristics of non-porous or macroporous (pore size > 50 nm) solids. Generally, Type I is obtained from microporous (pore size < 2 nm) solids. The adsorption takes place at very low relative pressure regions (ratio between the pressure and saturation pressure ($P/P_0 < 0.3$) due to multidirectional interactions between the pore walls and adsorbate. The Type IV isotherm is obtained using mesoporous (2 nm < pore size < 50 nm) solids. The hysteresis loop is associated with the secondary process of capillary condensation, which results in complete filling of the mesopores at $0.4 < P/P_0 < 1$.

This suggests that the prepared porous carbons have a broad pore size distribution. In the case of M-700, M-800, M-900 and M-1000, the knees of the isotherms at approximately $P/P_0 = 0.01$ are sharper than those of the isotherms of M-0 and M-500. The micropore structure develops significantly in the samples with increasing carbonization temperature. In the case of M-700 and M-1000, the isotherms showed an abrupt increase at $P/P_0 > 0.6$. Usually, the purpose of carbonization process is to increase the carbon content and to enrich the carbon porosity in the carbon precursors. There are several critical parameters in the preparation of porous carbons that would affect its structure, one of which is carbonization temperature. In the case where MgO nanoparticles was used, thermoplastic acrylic resin wetted very well on the surface of MgO to form thin films and decomposed above 200 °C to carbonaceous layer on the surface of MgO nanoparticles.[26]

During carbonization, most of the non-carbon elements, hydrogen and oxygen are first removed in gaseous form by pyrolytic decomposition of thermoplastic acrylic resin, and the free atoms of elementary carbon are grouped into organized crystallographic formations known as elementary graphite crystallites and wetted very well on the surface of MgO. Especially, carbonization temperature as the important parameters determines the quality and the properties of the final product.[20] The high carbonization temperature would result in a great amount of volatiles being released from the raw material and eventually influences the product yield and porosity. The results suggest that the prepared nanoporous carbons have large mesopores with a broad size distribution

Table 1. Pore structure parameters for the prepared nanoporous carbons from N_2 adsorption isotherms as the function of carbonization temperature

Samples	S_{BET}[a] (m^2/g)	V_{Micro}[b] (cm^3/g)	V_{Meso}[c] (cm^3/g)	V_{Total}[d] (cm^3/g)	F_{Micro}[e] (%)	D[f] (nm)
M-0	22	0.001	0.023	0.024	4.2	4.5
M-500	237	0.056	0.186	0.242	23.1	4.1
M-700	594	0.178	0.352	0.530	33.6	3.6
M-800	761	0.259	0.168	0.427	60.7	2.2
M-900	1251	0.400	0.230	0.630	63.5	2.1
M-1000	1067	0.235	0.528	0.763	30.8	2.9

[a]Specific surface area (m^2/g): BET equation ($P/P_0 = 0.05\text{-}0.1$). [b]Micropore volume (cm^3/g): Dubinin-Radushkevich equation. [c]Mesopore volume (cm^3/g): BJH equations. [d]Total pore volume (cm^3/g): V_{ads} ($P/P_0 = 0.995$) × 0.001547. [e]Fraction of micropore (%). [f]Average pore diameter (nm): $2 \times S_{BET}/V_{ads}$.

at high temperature. In addition, the specific surface area of the nanoporous carbons was enhanced significantly using MgO as a template and increasing the carbonization temperature.[26-28]

Table 1 lists the textural properties of the nanoporous carbon obtained at different carbonization temperatures. The specific surface area, micropore volume, mesopore volume, total pore volume, micropore pore volume ratio and mean pore diameter of the prepared porous carbon materials were estimated from the adsorption isotherms of N_2. As shown in Table 1, the specific surface area and total pore volume are dependent on the MgO-template and carbonization temperature. The specific surface area and micropore volume increased to M-900, and then decreased to M-1000. On the other hand, the total pore volume and mesopore volume of the carbon materials increased with increasing carbonization temperature, except at M-800. Moreover, the mean pore diameter of the porous carbons decreased to M-900, and then increased to M-1000. In particular, the M-900 sample exhibits values as high as 1201 m^2/g and 0.630 cm^3/g, which are higher than those of the porous carbon materials obtained using other templates.[29] The important parameters that determine the quality and the yield of the carbonized product are: (a) rate of heating, (b) final temperature, and (c) soaking time. In generally, the basic microstructure of the char with microporosity is formed around 500 °C. Some of these pores are blocked by the tarry products evolved during pyrolysis and could be available only when further heat treatment to about 800 °C is given. Further heat treatment to temperature of 1000 °C and above normally lead to hardening of the carbon structure due to partial alignment of graphitic planes and decrease in porosity which decelerate activation.[30] In this work, the micropore volume of nongraphiting carbons increases at low carbonization temperatures but decreases at higher temperatures due to thermal
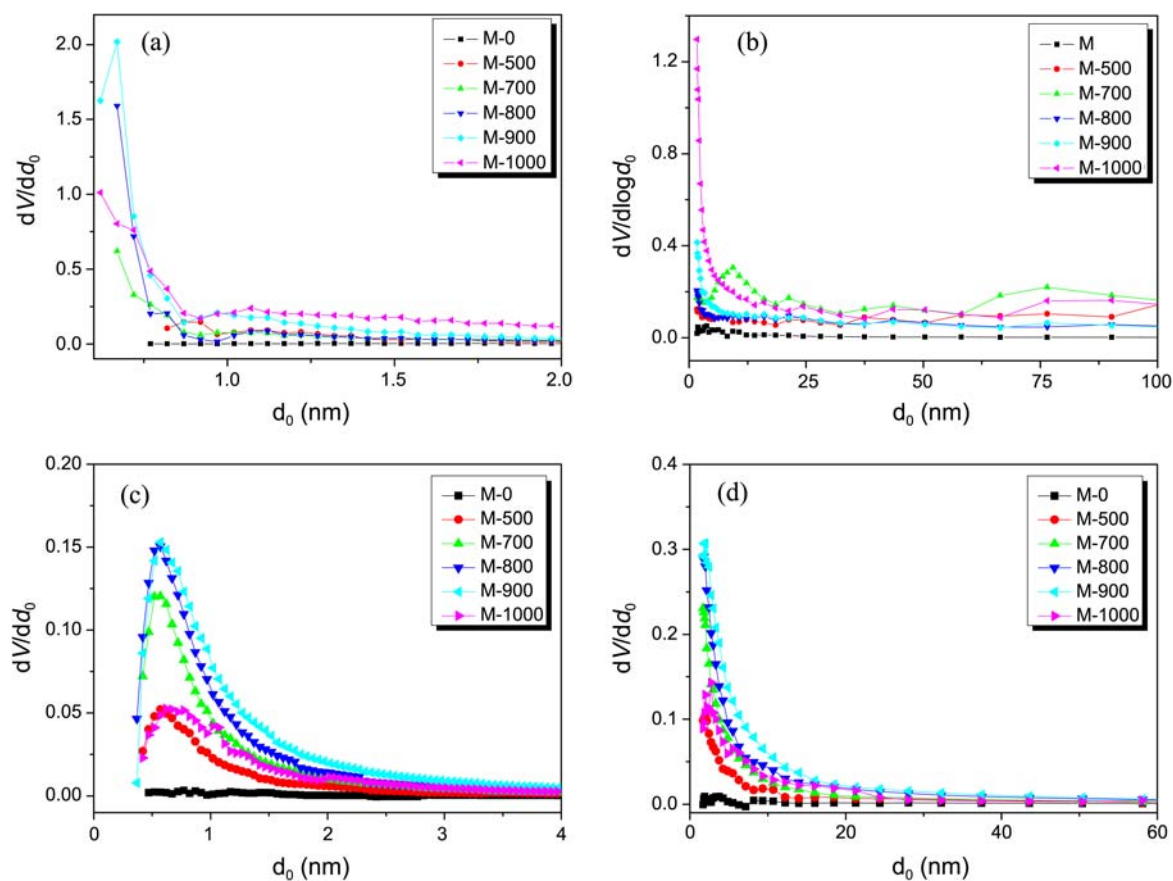
Figure 2. Micropore size distributions (a: $N_2/-196$ °C, c: $CO_2/0$ °C) and mesopore size distributions (b: $N_2/-196$ °C, d: $CO_2/0$ °C) of the prepared nanoporous carbons as function of the carbonization temperature.

shrinkage when MgO was used. The thermoplastic acrylic resin itself is known to give a graphitizing carbon, and the movement of thermoplastic acrylic resin is strongly disturbed on MgO surface during further pyrolysis. In addition, the shrinkage of carbon formed from thermoplastic acrylic resin is supposed to be strongly hindered in the thin film fixed on the surface of MgO during carbonization, which may leave micropores in the resultant carbon, and the formation of micropores on the wall of mesopores at lower carbonization temperature. Thus the present of MgO template and the carbonization temperature can be the factors controlling the pore structure of the carbons.[26-28]

Figure 2 shows the pore size distribution in the micro-/meso-pore region for better characterization of the change in the pore structure of the nanoporous carbon materials studied. To demonstrate the feasibility of such analysis and its consistency with the results for other gases, the isotherms of N_2 and CO_2 were measured at −196 °C and 0 °C respectively, on the prepared porous carbons. The micro-(Figure 2(a), (c)) and meso-(Figure 2(b), (d)) pore size distribution of the prepared nanoporous carbons at different carbonization temperatures were determined using the Horvath-Kawazoe (H-K) and Barrett-Joyner-Halenda (BJH) methods, respectively. The N_2 isotherms measured for these porous carbons and the corresponding pore size distributions calculated from the isotherms are shown in Figure 2(b). As shown in Figure 2(a), the micropore structures were enhanced predominantly by the carbonization of a mixture of MgO particles and resin in an inert atmosphere at higher temperatures, whereas the distributions indicate slight development around the micro region (0.62-0.12 nm). This confirms that the micropore development of the prepared porous carbon occurs mainly in the regions where the pore diameter is lower 0.92 nm, and the higher carbonization temperature (800 °C or 900 °C) favors the formation of a narrow micropore distribution.

As shown in Figure 2(b), the nanoporous carbons consist mainly of mesopores (< 80 nm) in diameter. The thermoplastic resin coats MgO particles, followed by its pyrolysis on the surface of MgO. The pore structures were enhanced predominantly by carbonization with MgO, and the pore size distributions showed that slight development can be observed around the narrow meso region. In addition, the number of narrow mesopores (< 14 nm) increased with increasing carbonization temperature. According to the literature, carbonization of a polymer with MgO plus heat treatment led to a change in the pore size distribution.[30]

Generally, the pore size distribution of a porous solid is evaluated from the analysis of N_2/−196 °C adsorption isotherms. However, that at this temperature diffusion of N_2 molecules into carbon micropores is very slow and diffusion limitations might influence adsorption in ultra-micropores (pores smaller than 0.7 nm). Thus, this type problem can be eliminated by using H_2, CO_2, and Ar adsorption analysis.[31] The pore size distributions obtained from such analyses for the samples (Figure 2(c)) show that the two methods give practically different results. In general, CO_2/0 °C molecules

can more easily access ultra-micropores than N_2/−196 °C. Jagiello *et al.* reported that CO_2 adsorption isotherm can be more easily measure the micropore size distribution at about initial pressure ($P/P_0 \sim 1$ Torr) and it is more convenient and beneficial to use CO_2/0 °C rather than N_2/−196 °C or Ar/−196 °C.[31] The results showed that analysis with CO_2 molecule at 0 °C shows the highest volumes for pores in the range below 0.57 nm for sample M-900. This suggests that this sample (M-900) has a narrow micropore size distribution.

This suggests that the porous structure of the obtained nanoporous carbons is strongly dependent on the change in carbonization temperature. With increasing temperature, more volatiles in samples would be released, causing a lower yield of resin. These findings are consistent with the general concept that increasing the carbonization temperature decreases the amount of the unstable volatiles on the carbon samples.

A marked increase in the number of narrow mesopores was attributed to decreases the amount of the unstable volatiles from the carbon precursors. The external pore structure of the prepared porous carbon materials was observed by SEM and TEM. Figure 3 shows typical SEM images of the resin and porous carbons. Figure 3(a) shows the carbonizaed resin. After carbonization at 900 °C, the morphology of the resin were disintegreated. When carbonization was
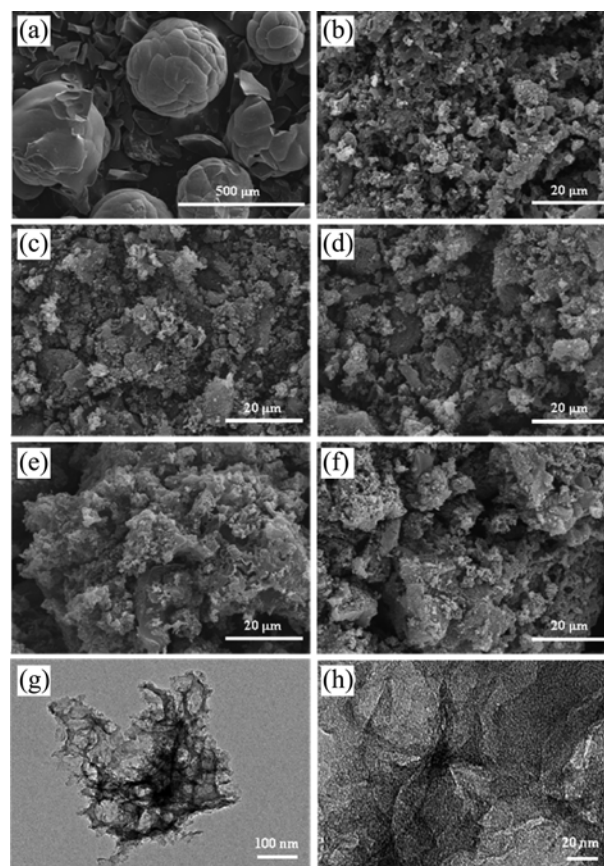

Figure 3. SEM (a-d) and TEM (e, f) images of the cation exchange resin (a), AM (b), and the prepared nanoporous carbon (c-h, M-900).

carried out at 900 °C for 2 h, the MgO particles appeared to have a marked effect, as shown in Figure 3(b-f). The resulting porous carbons prepared from the MgO-template method had a well-developed pore structure and a significantly different external surface morphology at different carbonization temperatures. Figure 3(g, h) show the texture of the micro-/mesoporous cores, which have a diameter of approximately 5-50 nm. The resin was mixed with MgO particles, followed by carbon precursor pyrolysis on the MgO surface. The powder contained a number of pores with a similar size and morphology of the MgO used (as shown in Figure 3 h). The N_2 isotherms, SEM and TEM show that this porous carbon has a hierarchical porous structure, *i.e.*, contains both mesopores and micropores.

The CO_2 adsorption capacity of the porous carbons was measured using CO_2 adsorption isotherms at 298 K, as shown in Figure 4. As shown in the figure, the MgO-template nanoporous carbons showed better performance for CO_2 adsorption than M-0. This clearly indicates that the resin produced by MgO-template carbonization temperature increases the affinity of the porous carbons towards CO_2. In addition, the adsorbed weights (CO_2) of all the carbon materials in the low relative pressure range were in the following order: M-900 > M-800 > M-700 > M-1000 > AM-500 > M-0, as shown in Figure 4. This is because the M-900 sample has a higher volume of narrow micropores than the other samples and hence a narrower pore size distribution, as shown in Figure 2(a). Sevilla *et al.* have been successfully prepared highly porous N-doped carbon as CO_2 sorbents that exhibits a CO_2 adsorption capacity of 194 mg/g at 298 K and 1 bar.[32] This suggests that the CO_2 adsorption capacity of the prepared nanoporous carbons was higher than that reported by Sevilla under similar conditions.

The adsorbed weights (CO_2) of all of the carbons species at a high relative pressure range were in the following order: M-1000 > M-900 > M-800 > M-700 > M-500 > M-0, as shown in Figure 5. In the relative pressure region, M-800 showed a maximum CO_2 adsorption capacity of 757 mg/g
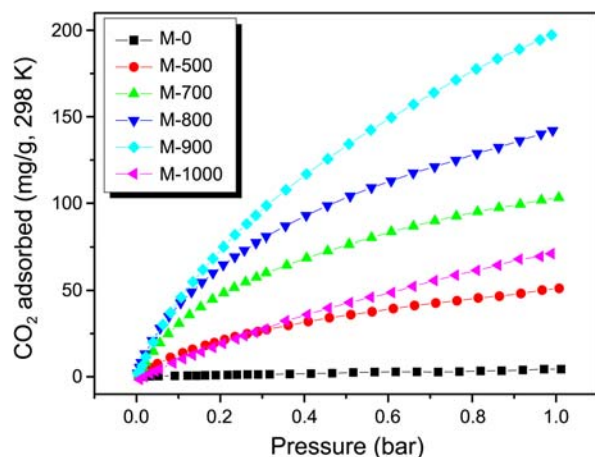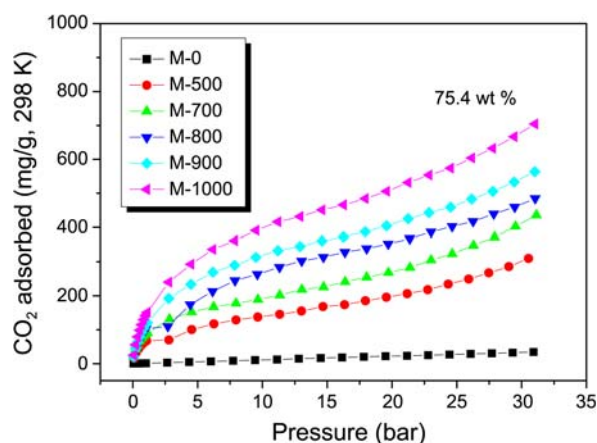

Figure 5. CO_2 adsorption isotherms of the prepared nanoporous carbons as function of the carbonization temperature measured at 30 bar.

(*Pressure* = 30 bar). The pore distribution is a key factor in developing a carbon material with a higher CO_2 adsorption capacity. The fact that M-1000 takes up more CO_2 at 30 bar is due to condensation in the space available within the mesopores. As the pressure was increased, the physical properties of the adsorbent, such as the specific surface area and micropore volume become increasingly important for CO_2 adsorption. This is because a high micropore volume means more adsorption sites available and a large pore volume means that there is more space available for CO_2 capture.

The room-temperature CO_2 adsorption of isotherms of activated graphite nanofibers (GNF-A), mesoporous silica (SBA-15), M-900, activated carbon fibers (ACFs), commercial activated carbons (ACs), mesoporous carbons (CMK), and muilti-wall carbon nanotubes (MCNTs) shown in Figure 6. The CO_2 adsorption isotherms of show no hysteresis, that indicates total reversibility in the take-up of CO_2. In the case of M-900, ACFs, ACs, CMK, and GNF-A, the CO_2 adsorption does not approach saturation even at a pressure of 1 bar

Figure 4. CO_2 adsorption isotherms of the prepared nanoporous carbons as function of the carbonization temperature measured at 1 bar.
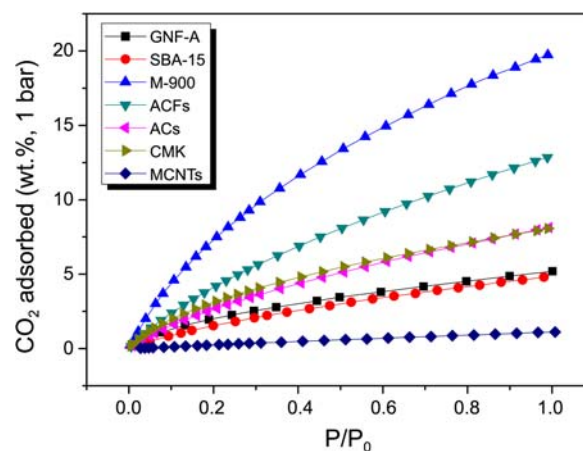

Figure 6. The CO_2 adsorption of isotherms of activated graphite nanofibers (GNF-A), mesoporous silica (SBA-15), M-900, activated carbon fibers (ACFs), commercial activated carbons (ACs), mesoporous carbons (CMK), and muilti-wall carbon nanotubes (MCNTs) at 25 °C and 1 bar.

Table 2. Pore structure parameters of activated graphite nanofibers (GNF-A), mesoporous silica (SBA-15), activated carbon fibers (ACFs), commercial activated carbons (ACs), mesoporous carbons (CMK), and muilti-wall carbon nanotubes (MWCNTs)

Samples	S_{BET}^{a} (m^2/g)	V_{Micro}^{b} (cm^3/g)	V_{Total}^{c} (cm^3/g)	F_{Micro}^{d} (%)	D^{e} (nm)	CO_2 wt %
CNF-A	567	0.274	0.708	38.7	5.0	5.2
SBA-15	435	0.029	0.533	5.4	4.9	4.8
M-900	1251	0.400	0.630	63.5	2.1	19.4
ACFs	1160	0.493	0.653	75.5	2.3	12.9
ACs	1453	0.050	1.382	3.6	3.8	8.1
CMK	1116	0.077	1.334	5.8	4.8	8.0
MWCNTs	209	0.030	0.610	4.9	11.7	1.1

[a]Specific surface area (m^2/g): BET equation ($P/P_0 = 0.05$-0.1). [b]Micropore volume (cm^3/g): Dubinin-Radushkevich equation. [c]Total pore volume (cm^3/g): V_{ads} ($P/P_0 = 0.995$) × 0.001547. [d]Micropore volume (cm^3/g): Dubinin-Astakhov equation. [e]Average pore diameter (nm): $2 \times S_{BET}/V_{ads.}$

implying that even greater adsorption capacities are possible at even higher pressures. The sample prepared at 900 °C (M-900) exhibits the highest CO_2 adsorption capacity. Recently, several authors have investigated that adsorbents with a large population of pores of size 1-2 nm exhibit a better CO_2 adsorption performance than those with narrower micropores or with a mesoporous pore network.[33-35] Table 2 lists the textural properties of these porous materials. The efficient adsorbents would be required at low partial pressures, such as those for CO_2 adsorption in post-combustion flue gas streams (~0.1 bar). As shown in Figure 6, the adsorbed weights (CO_2) of all of the porous materials range at low partial pressure were in the following order: M-900 > ACFs > CMK > ACs > GNF-A > SBA-15 > MCNTs.

According to Table 2, the trend in CO_2 adsorption capacity is clearly related to the larger microporosity, the improved adsorption capacities being a result of the improved supermicroporosity (< 2 nm) that prepared carbons. The supermicroporosity of M-900 are those with the free passage of pores smaller than the bilayer thickness of typical adsorptive, CO_2 molecular (kinetic diameter, 0.33 nm at 25 °C).[34,35] In the case of M-900, CO_2 molecules diffused inside the supermicropore channels because the free openings are larger than the kinetic diameters of CO_2 molecules.

Conclusions

The results presented in this work show that a large enhancement for CO_2 capture by carbonizing the mixture of thermoplastic acrylic resin and MgO particles at 500-1000 °C. The specific surface area and CO_2 adsorption capacity of the obtained porous carbons increased significantly with increasing carbonization temperature. At higher temperature, enhancement may be attributed mainly to the very narrow microporosity. The CO_2 adsorption capacity (194 mg/g) of prepared porous carbons (at 900 °C) is higher than widely used porous materials at 25 °C and 1 bar. The specific surface area increased from 237 to 1251 m^2/g, and the total pore volume rose from 0.242 to 0.763 cm^3/g.

References

1. Haszeldine, R. S. *Science* **2009**, *325*, 1647.
2. Williams, J. H.; DeBenedictis, A.; Ghanadan, R.; Mahone, A.; Moore, J.; Morrow, W. R., III; Price, S.; Torn, M. S. *Science* **2012**, *335*, 53.
3. Reay, D. S.; Dentener, F.; Smith, P.; Grace, J.; Feely, R. A. *Nature Geosci.* **2008**, *1*, 430.
4. International Energy Agency, Tracking industrial energy efficiency and CO_2 emissions, OECD/IEA, Paris, 2007.
5. Samanta, A.; Zhao, A.; Shimizu, G. K. H.; Sarkar, P.; Gupta, R. *Ind. Eng. Chem. Res.* **2012**, *51*, 1438.
6. Aaron, D.; Tsouris, C. *Sep. Sci. Technol.* **2005**, *40*, 321.
7. Rochelle, G. T. *Science* **2009**, *325*, 1652.
8. Zhang, Y.; Que, H.; Chen, C. C. *Fluid Phase Equil.* **2011**, *311*, 67.
9. Versteeg, P.; Rubin, E. S. *Inter. J. Greenhouse Gas Control* **2011**, *5*, 1596.
10. Sevilla, M.; Fuertes, A. B. *J. Colloid Interface Sci.* **2012**, *366*, 147.
11. Nachtigall, P.; Grajciar, L.; Pérez-Pariente, J.; Pinar, A. B.; Zukal, A.; Čejka, J. *Phys. Chem. Chem. Phys.* **2012**, *14*, 1117.
12. Abid, H. R.; Pham, G. H.; Ang, H. M.; Tade, M. O.; Wang, S. *J. Colloid Interface Sci.* **2012**, *366*, 120.
13. Morishige, K. *J. Phys. Chem.* **2011**, *115*, 9713.
14. Nicolas, C. H.; Sublet, J.; Schiirman, Y.; Pera-Titus, M. *Chem. Eng. Sci.* **2011**, *66*, 6057.
15. Modak, A.; Nandi, M.; Mondal, J.; Bhaumik, A. *Chem. Commun.* **2012**, *48*, 248.
16. Meng, L. Y.; Cho, K. S.; Park, S. J. *Carbon Lett.* **2009**, *10*, 221.
17. Kim, B. J.; Cho, K. S.; Park, S. J. *J. Colloid Interface Sci.* **2010**, *342*, 575.
18. Pevida, C.; Plaza, M. G.; Arias, B.; Fermoso, J.; Rubiera, F.; Pis, J. J. *Appl. Surf. Sci.* **2008**, *254*, 7165.
19. Meng, L. Y.; Cho, K. S.; Park, S. J. *Carbon Lett.* **2010**, *11*, 34.
20. Meng, L. Y.; Park, S. J. *J. Colloid Interface Sci.* **2010**, *352*, 498.
21. Mishra, A. K.; Ramaprabhu, S. *AIP Advances* **2011**, *1*, art. no. 032152.
22. Varghese, S. H.; Nair, R.; Nair, B. G.; Hanajiri, T.; Maekawa, T.; Yoshida, Y.; Kumar, D. S. *Curr. Nanosci.* **2010**, *6*, 331.
23. Zong, J.; Zhu, Y.; Yang, X.; Li, C. *J. Alloys Compounds* **2011**, *509*, 2970.
24. Jiang, X.; Ju, X.; Huang, M. *J. Alloys Compounds* **2011**, *509*, S864.
25. Sevilla, M.; Alam, N.; Mokaya, R. *J. Phys. Chem. C* **2010**, *114*, 11314.
26. Konnoa, H.; Onishia, H.; Yoshizawab, N.; Azumia, K. *J. Power Sources* **2010**, *195*, 667.
27. Morishita, T.; Soneda, Y.; Tsumura, T.; Inagaki, M. *Carbon* **2006**, *44*, 2360.
28. Morishita, T.; Ishihara, K.; Kato, M.; Inagaki, M. *Carbon* **2007**, *45*, 209.
29. Roldán, S.; Villar, I.; Ruíz, V.; Blanco, C.; Granda, M.; Menéndez, R.; Santamaría, R. *Energy Fuels* **2010**, *24*, 3422.
30. Manocha, S. M. *Sadhana* **2010**, *28*, 335.
31. Jagiello, J. M. *Carbon* **2004**, *42*, 1227.
32. Meng, L. Y.; Park, S. J. *J. Colloid Interface Sci.* **2012**, *366*, 125.
33. Sevilla, M.; Valle-Vigón, P.; Fuertes, A. B. *Adv. Funct. Mater.* **2011**, *21*, 2781.
34. Siriwardane, R. V.; Shen, M. S.; Fisher, E. P.; Poston, J. A. *Energy Fuels* **2001**, *15*, 279.
35. Hao, G. P.; Li, W. C.; Lu, A. H. *J. Mater. Chem.* **2010**, *21*, 6447.